Journal of Biomolecular NMR, **12:** 435–441, 1998.
KLUWER/ESCOM

Spin-state selection filters for the measurement of heteronuclear one-bond coupling constants

Patrik Andersson, Johan Weigelt and Gottfried Otting*
Department of Medical Biochemistry and Biophysics, Karolinska Institute, S-171 77 Stockholm, Sweden

Received 29 January 1998; Accepted 23 April 1998

Key words: α/β-HSQC, α/β-HSQC-α/β, DnaB, *E. coli* arginine repressor, HACACO-α/β, HSQC-α/β, one-bond coupling constants

Abstract

Novel α/β-half-filter elements are proposed for the separation of the high-field and low-field component of $^1J_{HC}$ and $^1J_{HN}$ splittings into different subspectra. The α/β-half-filter elements are of the same duration as the S^3CT pulse sequence element and, like this, are less sensitive to cross talk between different subspectra than the original shorter α/β-half-filters. The filter elements are demonstrated with the measurement of $^1J_{HC}$ coupling constants of $C^\alpha H$ groups in 2D and 3D experiments and the subspectral editing of the four different multiplet components observed in two-dimensional α/β-HSQC-α/β spectra recorded without heteronuclear decoupling in either dimension.

The separation of two doublet components into different subspectra provides a convenient way of measuring the coupling constant and can be achieved by spin-state selective experiments using exclusively non-selective pulses (Nielsen et al., 1996a,b; Ross et al., 1996; Sattler et al., 1996; Meissner et al., 1997a,b; Sørensen et al., 1997; Andersson et al., 1998). Furthermore, spin-state selective experiments allow the selection of the most slowly relaxing multiplet component in heteronuclear correlation experiments (Pervushin et al., 1997). This communication presents a new variant of spin-state selective filter elements, a brief comparison with existing filters, and experimental examples for the measurement of the scalar one-bond coupling constant $^1J_{HC}$ of $C^\alpha H$ groups in ^{13}C-enriched proteins.

The two doublet lines of a spin with a single coupling partner correspond to the α and β state of the coupling partner, respectively. For a two-spin system with the proton spin *I* and the heteronuclear spin *S*, the two doublet components can be described as the sum or difference of in-phase and antiphase magnetization, $I_y \pm 2I_yS_z$. Using spin-state selective experiments, the in-phase and antiphase magnetizations become available individually, allowing the separation of the two doublet components into different subspectra. Figure 1 shows a selection of filter elements by which this editing can be achieved.

All filter elements of Figure 1 can be used with $2I_yS_z$ as starting magnetization. Evolution under the scalar coupling J_{IS} leads to $2I_yS_z \cos(\pi J_{IS}\tau/2) - I_x \sin(\pi J_{IS}\tau/2)$. For $\tau = 1/(2J_{IS})$, both terms are of identical magnitude. In a vector description, the *I* spins bound to *S* spins in the state α or β, respectively, have precessed in opposite directions by 45° each. At this point, the S^3E pulse sequence uses two 90° pulses of either the same or opposite phase to invert or not invert the sign of one of the doublet components. If stored separately, the two data sets obtained in this way can be additively or subtractively combined to yield the different doublet components (Meissner et al., 1997a,b). The α/β-half-filter element of Figure 1B works in an analogous way, except that the two data sets differ by the presence or absence of the editing 180°(*S*) pulse inverting the sign of the antiphase magnetization term. The S^3E pulse sequence element and the α/β-half-filter yield the same results, if pulse imperfections can be neglected, except that the α/β-half-filter can start from *I* spin magnetization of

*To whom correspondence should be addressed: Gottfried Otting, Karolinska Institute, MBB, Doktorsringen 9A, S-171 77 Stockholm, Sweden, Tel: +46-8-728 6804. Fax: +46-8-335296. E-mail: gottfried.otting@mbb.ki.se.

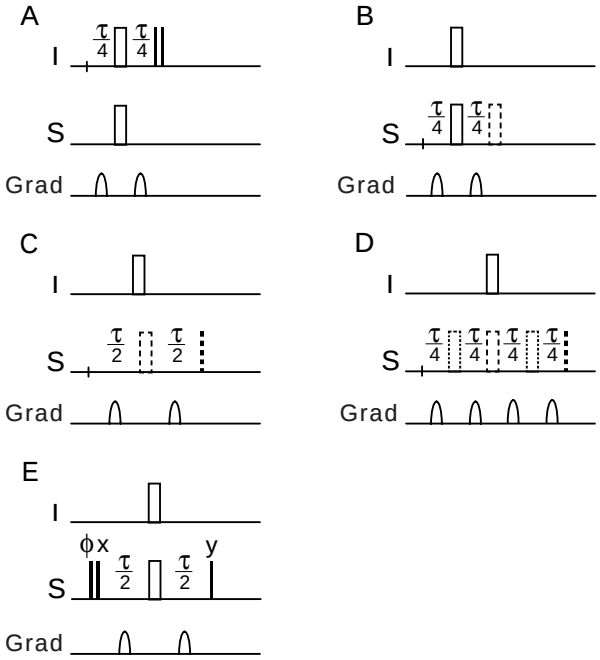

Figure 1. Pulse sequence elements for spin-state selection. Starting from transverse antiphase magnetization $2I_yS_z$, these pulse sequences are sufficient to edit the two doublet components of the I spin in an $I-S$ two-spin system into two different one-dimensional subspectra. The filter elements (A) to (D) can equally well be used starting from in-phase magnetization I_y. Narrow (wide) bars represent pulses with flip angles of 90° (180°). Dashed lines indicate editing pulses applied only every second scan. $\tau = 1/(2J_{IS})$. (A) S^3E pulse sequence element. The 90°(I) pulses are phase shifted by 45° with respect to the starting magnetization. Two data sets are recorded with different phase cycles, yielding the two subspectra by addition and subtraction (Meissner et al., 1997a,b). (B) Short α/β-half-filter. Two data sets are recorded with and without the editing 180°(S) pulse. The two subspectra are obtained by addition and subtraction, followed by phase shifting of one of the resulting data sets by 90°, and addition and subtraction of these new data sets (Andersson et al., 1998). (C) Long α/β-half-filter. Two data sets are recorded with and without the editing 180°(S) pulse. In addition, the 90°(S) pulse is applied only in the scans selecting in-phase I spin magnetization. The two subspectra are obtained by addition and subtraction of the recorded data sets. (D) Long α/β-half-filter with averaging of the relaxation rates of both doublet components in the presence of cross-correlation between dipole-dipole and CSA relaxation. Two data sets are recorded with the 180°(S) pulse shown by dashed lines or with the 180°(S) pulses indicated by dotted lines. In (C) and (D) the 90°(S) pulse is applied only in the scans selecting in-phase magnetization. (E) S^3CT pulse sequence element for the editing of doublet components starting from antiphase magnetization $2I_xS_z$ or $2I_yS_z$. Two data sets are recorded with different phase ϕ, yielding the two subspectra by addition and subtraction (Sørensen et al., 1997).

arbitrary phase, as encountered, for example, in phase encoded experiments using pulsed field gradients for coherence selection (Andersson et al., 1998). The α/β-half-filter element can lead to imperfect subspectral editing, if inversion by the editing 180° pulse is incomplete. In the S^3E pulse sequence element, signal is lost by chemical shift evolution during the pair of 90°(I) pulses (Zerbe et al., 1992).

If the total filter delay τ/2 does not exactly match $1/(4J_{IS})$, some residual signal from one subspectrum also appears in the other subspectrum. The new α/β-half-filter elements shown in Figures 1C and D are less sensitive to variations in scalar coupling constants. Two data sets with and without effective decoupling of the J_{IS} coupling are recorded. The total filter delay τ corresponds to $1/(2J_{IS})$. Starting from antiphase magnetization $2I_yS_z$, the filter element of Figure 1C yields unmodified antiphase magnetization in the absence of the 180°(S) pulse. With this editing pulse, in-phase magnetization I_x is obtained. Any residual antiphase magnetization is purged by the 90°(S) pulse which is applied only in the scans selecting in-phase magnetization. Two different data sets are thus obtained, containing pure in-phase and antiphase magnetization, respectively. After phase shifting one of the data sets by 90°, for example by swapping the real and imaginary parts of each complex data point, the two data sets can be added or subtracted to yield the subspectra containing one or the other doublet component. The sensitivity of the α/β-half-filter element of Figure 1B towards J mismatch is the same as that of the S^3E pulse sequence element (Figure 1A). The sensitivity of the new α/β-half-filter elements of Figures 1C and D towards J mismatch is the same as that of the S^3CT pulse sequence element (Figure 1E). Plots of the intensities of the desired and undesired components as a function of $\Delta J/J_0$ ($\tau = (2J_0)^{-1}$) in subspectra of S^3E and S^3CT experiments have been shown previously (Figure 6 in Sørensen et al., 1997). The α/β-half-filter element of Figure 1D differs from that of Figure 1C by the presence of two 180°(S) pulses in the middle of the delays τ/2, when the data set with J_{IS} decoupling is recorded. This averages the relaxation rates of the two doublet components of the I spin, when they relax with different rates due to cross-correlation between dipole-dipole and CSA relaxation (Goldman, 1984). A direct comparison of the α/β-half-filters with the S^3CT element is complicated by the fact that the latter was designed to achieve coherence transfer at the same time as spin-state selection. Thus, the S^3CT element requires antiphase magnetization at the start.

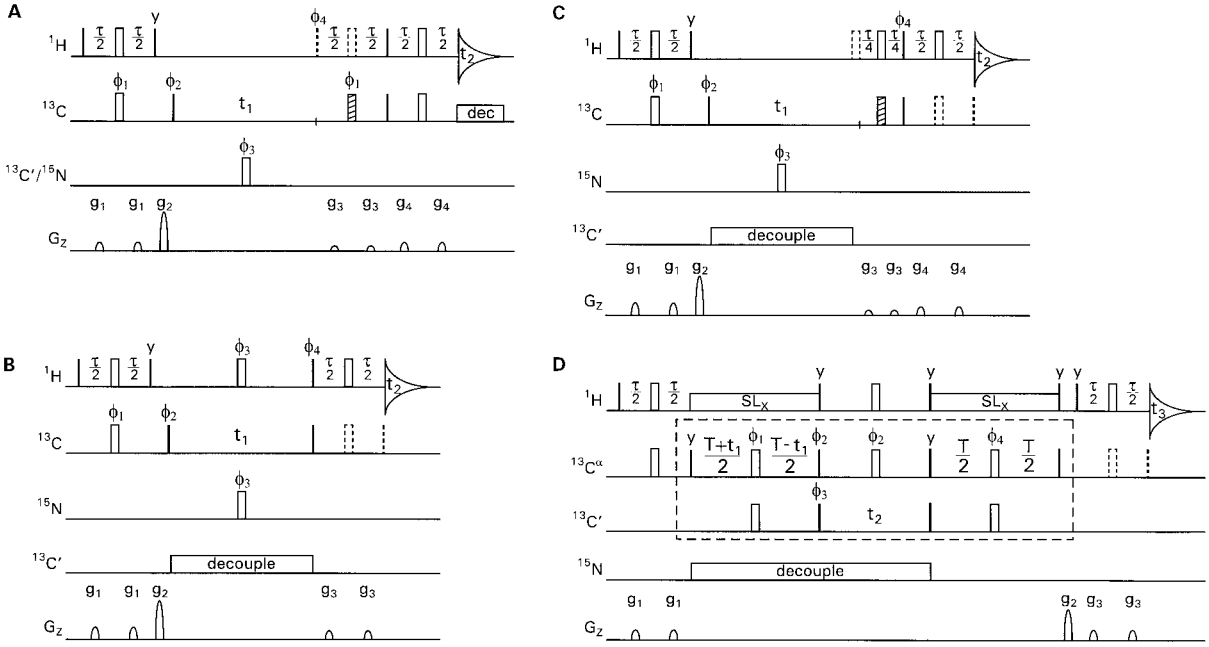

Figure 2. Pulse sequences for the subspectral editing of the multiplet components of $^{13}C-^{1}H$ cross peaks of $C^{\alpha}H$ groups. $\tau = 1/(2^{1}J_{HC}) = 3.45$ ms. Hatched bars denote rectangular 180°(^{13}C) pulses applied at 55 ppm with a duration of 47 μs to avoid excitation of the carbonyl resonances. All pulses, except where noted, are applied with phase x. All pulsed field gradients were applied with a sine-bell shape and a duration of 500 μs and followed by a recovery delay of at least 300 μs. Carbonyl resonances were decoupled either by a 1.0 kHz SEDUCE sequence (McCoy and Mueller, 1992) or by 47 μs 180°(^{13}C) pulses applied at 176 ppm. (A) α/β-HSQC. For subspectral editing, two data sets are recorded with and without the editing 180°(^{1}H) pulse drawn with dashed lines, and recombined as described in Figure 1C. The 90°(^{1}H) pulse drawn with a dashed line is applied in the scans with the editing 180°(^{1}H) pulse. Phase cycle: $\phi_1 = x$; $\phi_2 = x, -x$; $\phi_3 = \phi_4 = 2(x), 2(-x)$; receiver $= x, -x$. Gradient strengths: $g_{1,2,3,4} = 2.5, 11.0, 1.5, 2.5$ G/cm. (B) HSQC-α/β. For subspectral editing, two data sets are recorded as in (A). Phase cycle: $\phi_1 = x$; $\phi_2 = x, -x$; $\phi_3 = 2(x), 2(-x)$; $\phi_4 = 4(x), 4(-x)$; receiver $= 2(x, -x), 2(-x, x)$. Gradient strengths: $g_{1,2,3} = 3.5, 11.0, 2.5$ G/cm. (C) α/β-HSQC-α/β with short and long α/β-half-filters in the t_1 and t_2 dimension, respectively. For subspectral editing, the following four data sets (I to IV), are recorded: (I) with the editing pulses in both α/β-half-filters; (II) with editing 180°(^{1}H) pulse in the first α/β-half-filter, and without editing 180°(^{13}C) and 90°(^{13}C) pulses in the second; (III) without editing 180°(^{1}H) pulse in the first α/β-half-filter, and with editing 180°(^{13}C) and 90°(^{13}C) pulses in the second; (IV) without editing pulses in either α/β-half-filter. The four subspectra can be obtained by the following procedure: first, the data sets II and IV are phase shifted by 90° in the t_2 dimension to yield the data sets II_{90} and IV_{90}, e.g. by exchanging the real and imaginary parts of each complex data point; next, four new data sets are calculated to select the high-field and low-field doublet component in the F_2 dimension: a = I + II_{90}; b = I − II_{90}; c = III + IV_{90}; d = III − IV_{90}. Each pair of data sets, a and c, and b and d, is subsequently rearranged as described in Figure 1B to achieve the editing in the F_1 dimension. Phase cycle: $\phi_1 = x$; $\phi_2 = x, -x$; $\phi_3 = 2(x), 2(-x)$; $\phi_4 = 4(x), 4(-x)$; receiver $= 2(x, -x), 2(-x, x)$. Gradient strengths: $g_{1,2,3,4} = 3.5, 11.0, 1.5, 2.5$ G/cm. Quadrature detection in the indirect frequency dimension is achieved by simultaneously incrementing the phases ϕ_1 and ϕ_2 with the evolution time t_1. (D) HACACO-α/β pulse sequence. Subspectral editing as in (A). $T = 7$ ms. Phase cycle: $\phi_1 = 4(x), 4(y), 4(-x), 4(-y)$; $\phi_2 = 2(x), 2(-x)$; $\phi_3 = x, -x$; $\phi_4 = x$; receiver $= x, -x, -x, x, -x, x, x, -x$. Gradient strengths(durations): $g_{1,2,3} = 4.0$ G/cm (0.5 ms), 8.5 G/cm (1.0 ms), 3.0 G/cm (0.5 ms). ^{13}C pulses were non-selective, except for the pulses within the dashed box which were applied with durations of 53 μs and 47 μs for 90° and 180° pulses, respectively, to minimize mutual excitation of C^{α} and C′ resonances. $^{13}C'$ pulses were applied immediately after or before the corresponding $^{13}C^{\alpha}$ pulses, although displayed as simultaneous in the figure. For optimum sensitivity, off-resonance effects of the 180°($^{13}C'$) pulses were compensated by adding an experimentally determined, constant phase offset to ϕ_1 and ϕ_4 (Grzesiek and Bax, 1993). The $^{1}H^{\alpha}$ spin-locking field was applied with an RF strength of 6.25 kHz.

Furthermore, the occurence of transverse S spin coherences during the S^3CT element requires different filter delays for CH, CH_2 and CH_3 groups ($I = ^{1}H$, $S = ^{13}C$), and causes complications in the presence of $^{1}J_{CC}$ couplings (Ross et al., 1996), whereas the same α/β-half-filter delay is optimum for all these spin systems, as only I spins evolve. Compared to the S^3CT pulse sequence element of Figure 1E, the α/β-half-filter elements of Figures 1C and D have the advantage that the 180°(S) pulses in the middle of the filter delays exclusively serve for inversion rather than refocusing, allowing the use of simple composite or adiabatic pulses for the optimum inversion of large spectral widths. Homonuclear I spin couplings evolv-

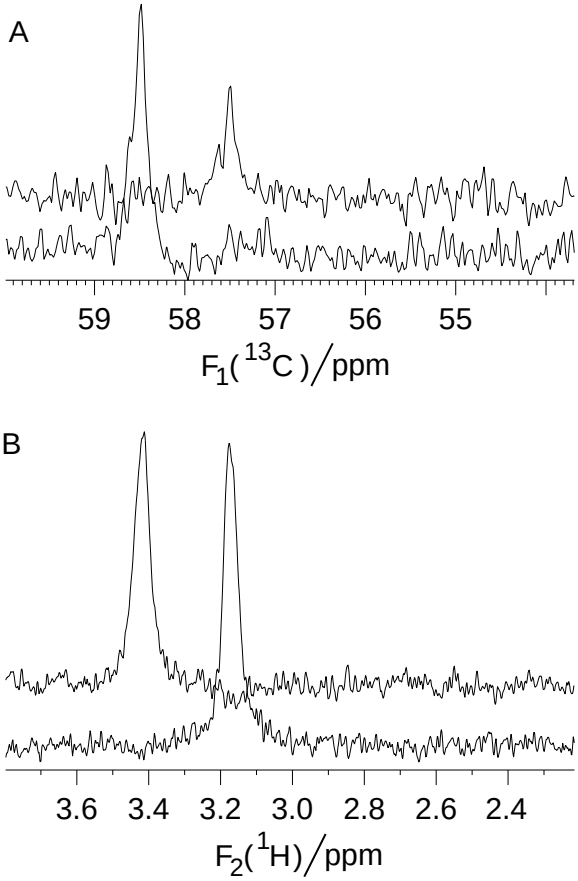

Figure 3. Cross sections through subspectra of α/β-HSQC and HSQC-α/β experiments recorded with a 3 mM solution of 30% ^{13}C/100% ^{15}N labelled 78 residue N-terminal domain of *E. coli* arginine repressor at 28 °C, pH 5.5. The cross sections show the doublet components of the $^{13}C-^{1}H$ cross peak of Leu10 $C^{\alpha}H$ for which $^{1}J_{CH}$ = 148 Hz. (A) Cross sections through the subspectra of the α/β-HSQC experiment recorded with the pulse sequence of Figure 2A. Parameters: τ = 3.45 ms, t_{1max} = 154 ms, t_{2max} = 170 ms, total experimental time 3 h, Bruker DMX-600 NMR spectrometer. Before Fourier transformation, the data were multiplied by cosine and cosine squared window functions in the t_1 and t_2 dimension, respectively. Corresponding data recorded with the α/β-half-filters of Figure 1B and Figure 1D gave very similar spectra (data not shown). (B) Cross sections through the subspectra of the HSQC-α/β experiment recorded with the pulse sequence of Figure 2B. Parameters: t_{1max} = 50 ms, t_{2max} = 341 ms, total experimental time 7.5 h. Other parameters were identical to those in (A).

ing during the α/β-half-filter affect the line-shape of the *I* spin resonances only little, as in conventional half-filter experiments (Otting and Wüthrich, 1990).

Figure 2 shows implementations of the α/β-half-filter schemes in HSQC-type experiments as well as in a 3D HACACO experiment. The α/β-HSQC experiment of Figure 2A was designed for the separation of the doublet components of $^{13}C^{\alpha}-H^{\alpha}$ cross peaks in the F_1 frequency dimension. The efficiency of this experiment for measuring $^{1}J_{CH}$ couplings was compared to that of the HSQC-α/β experiment of Figure 2B, where the doublets are edited in the F_2 frequency dimension. The doubly-edited α/β-HSQC-α/β experiment of Figure 2C separates all four multiplet components of the $^{13}C^{\alpha}-H^{\alpha}$ cross peaks into different subspectra. The HACACO-α/β experiment of Figure 2D facilitates the measurement of $^{1}J_{CH}$ coupling constants when the corresponding cross peaks are overlapped in two-dimensional spectra.

Spectra using the pulse sequences of Figure 2A–C were recorded with a 30% ^{13}C/100%^{15}N labelled sample of the 78 residue amino terminal domain of the *E. coli* arginine repressor (Arg-N; Sunnerhagen et al., 1997) dissolved in D_2O. Figures 3A and B show a comparison of representative cross sections through the subspectra of α/β-HSQC and HSQC-α/β experiments. Although the $T_1(^{13}C)$ relaxation times of the $C^{\alpha}H$ groups are longer than the $T_1(^{1}H)$ relaxation times, the sensitivity and resolution is better in the HSQC-α/β subspectra (Figure 3B). Most notably, the high-field component of the doublet observed in the α/β-HSQC experiment is significantly broadened by cross-correlation between dipole-dipole relaxation and CSA relaxation of the ^{13}C spin (Goldman, 1984). In addition, $^{1}J_{CC}$ couplings broaden the multiplet in the cross sections of the α/β-HSQC experiment. Consequently, $^{1}J_{HC}$ couplings are easier to measure in the F_2 dimension of HSQC-α/β subspectra than in the F_1 dimension of α/β-HSQC subspectra.

Similar to experiments with regular half-filter elements (Otting and Wüthrich, 1989, 1990), the independent application of α/β-half-filters in the t_1 and t_2 evolution periods allows the generation of four subspectra. As an example, the implementation of two α/β-half-filter elements in an HSQC pulse sequence is shown in Figure 2C. Four data sets were recorded for this 'α/β-HSQC-α/β' experiment, with and without editing pulses of the α/β-half-filters. By appropriate combination of the data sets (see caption of Figure 2C), the four components of the $C^{\alpha}-H^{\alpha}$ cross peak were edited into four different subspectra (Figures 4A–D). When cross-correlation effects between the dipole-dipole and CSA relaxation significantly narrow the low-field components in the ^{13}C dimension, a spectrum selecting these multiplet components can have a better signal-height-to-noise ratio than a decoupled spectrum (Pervushin et al., 1997). For dou-

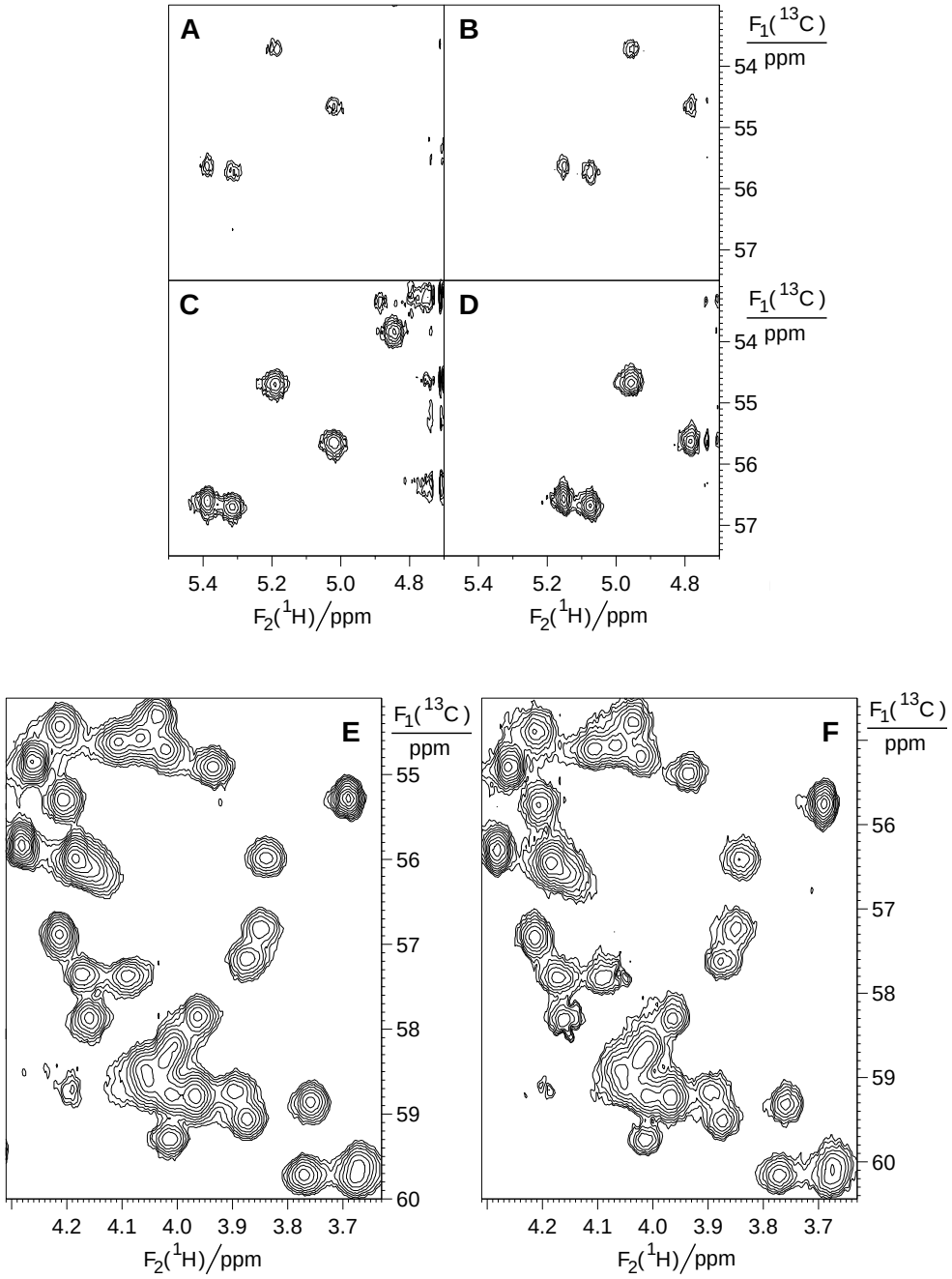

Figure 4. Subspectra of an α/β-HSQC-α/β experiment recorded with the N-terminal domain of *E. coli* arginine repressor and comparison with a subspectrum from the HSQC-α/β experiment of Figure 3B. The experiments were recorded with the pulse sequences of Figures 2C and 2B, respectively. The same sample was used for both experiments. Identical τ, t_{1max}, t_{2max}, total experimental time, window functions and plotting parameters were used. (A)–(D) Selected spectral region from the four subspectra of the α/β-HSQC-α/β experiment, each containing one of the four different multiplet components of the $^{13}C-^{1}H$ cross peaks of $C^{\alpha}H$ groups separated by $^{1}J_{CH}$ in both dimensions. Each contour level was plotted by a factor $\sqrt{2}$ above the preceding one. The noise band at $F_2 = 4.73$ ppm is from the residual HDO signal. (E) and (F) Comparison of subspectra from the HSQC-α/β (E) and α/β-HSQC-α/β (F) experiments. The subspectra contain the low-field component of the doublets in the F_2 dimension. In addition, the subspectrum of the α/β-HSQC-α/β experiment selects the low-field component of the doublet in the F_1 dimension. Note that the spectral region of the α/β-HSQC-α/β subspectrum was shifted in the F_1 dimension by about 75 Hz to show the multiplet components corresponding to the cross peaks in the HSQC-α/β subspectrum.

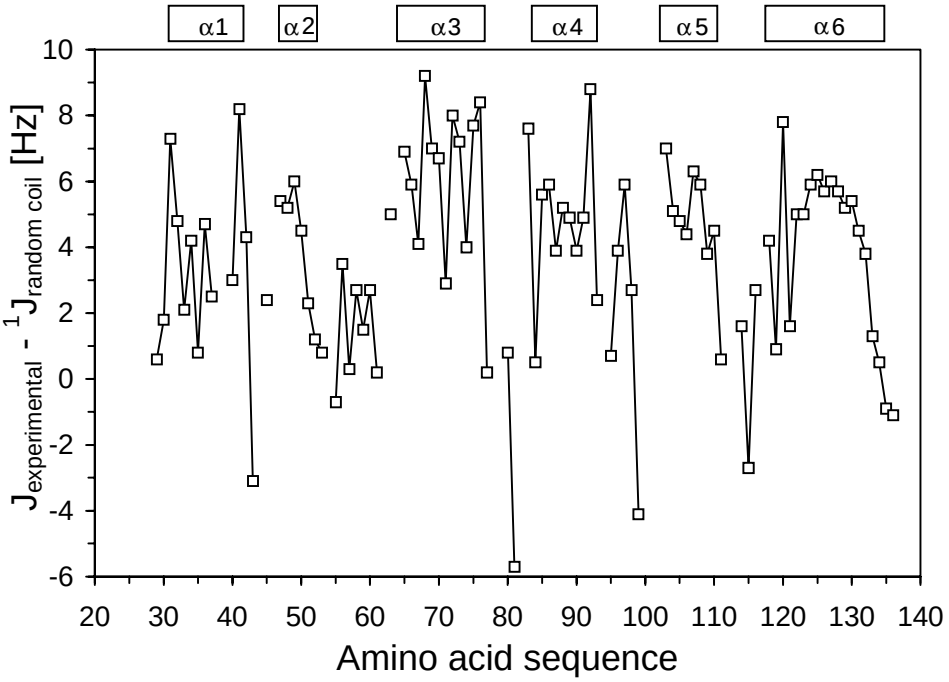

Figure 5. Difference between the $^1J_{HC}$ coupling constants of $C^\alpha H$ groups measured for the N-terminal domain of *E. coli* DnaB helicase using the HACACO-α/β experiment of Figure 2D, and random coil values by Vuister et al. (1993). The data were recorded with a 2 mM sample of DnaB(24-136) in D_2O (20 mM sodium phosphate buffer containing 1 mM EDTA and 0.02% w/v NaN_3) at pH 7.5, 32 °C. Spectral widths/number of complex data points: 4464 Hz/28 pts [F_1, $^{13}C^\alpha$], 1887 Hz/38 pts [F_2, $^{13}C'$] and 6776 Hz/1024 pts [F_3, ^1H]. The total acquisition time was 48 h. $^1J_{CH}$ values determined from different experiments correlated with an rms deviation of about 1 Hz. Values for glycyl residues and overlapping cross peaks are not plotted. The regular secondary structure elements identified by chemical shift indices and short range NOEs (Weigelt et al., 1998) are indicated at the top.

blets with Lorentzian lineshapes, the selection of the low-field component becomes worthwhile, when it relaxes three times more slowly than the high-field component. This limit was reached for several of the C^α-H^α cross peaks in the Arg-N sample. Figures 4E and F compare a representative spectral region in subspectra recorded with the HSQC-α/β and α/β-HSQC-α/β experiments of Figures 2B and C, respectively. Only the subspectra containing the low-field doublet component in the ^1H dimension are shown. In addition, the low-field doublet component was selected in the ^{13}C dimension of the doubly edited subspectrum (Figure 4F). Although the α/β-HSQC-α/β experiment was recorded without ^1H decoupling in the F_1 frequency dimension, it is for most cross peaks comparable in resolution and sensitivity to the HSQC-α/β subspectrum recorded with ^1H decoupling. Conceivably, the doubly edited α/β-HSQC-α/β experiment would be attractive at higher magnetic fields.

For larger proteins, homonuclear H^α-H^β couplings are no longer resolved in the $C^\alpha-H^\alpha$ cross peaks. Since conformation dependent cross-correlation effects affect the intensities of the individual, unresolved $^1H-^1H$ multiplet components differently for the two ^{13}C satellite signals (Cuperlovic et al., 1996), the $^1J_{CH}$ coupling constants are more accurately measured by comparing the separations of the bottom halves of the peaks rather than by measuring peak-to-peak separations. An HACACO-α/β experiment recorded with a sample of the 113 residue N-terminal domain of *E. coli* DnaB helicase, using the pulse sequence of Figure 2D, showed cross peaks with unresolved multiplet fine-structure, where the width of the envelope comprising each H^α multiplet typically was about 35 Hz. Nevertheless, the $^1J_{CH}$ values measured for the $C^\alpha H$ groups correlate well with the secondary structure elements predicted by NOEs and chemical shift indices (Figure 5; Weigelt et al., 1998). HACACO experiments with spin-locking of the H^α resonances (Figure 2D) were found to yield less t_1 noise than and comparable sensitivity to experiments using broadband decoupling of the H^α resonances (Grzesiek and Bax, 1993).

In conclusion, the new α/β-half-filters are versatile pulse sequence elements for spin-state selection.

Their reduced sensitivity towards coupling mismatch make them particularly attractive for the measurement of heteronuclear one-bond coupling constants varying over a greater range, for example because of dipolar contributions in partially oriented samples (Tjandra and Bax, 1997; Bax and Tjandra, 1997).

Acknowledgements

We thank Maria Sunnerhagen and Kerstin Nordstrand for the sample of labelled arginine repressor, and Sue Brown and Nicholas Dixon for the sample of labelled DnaB. P.A. acknowledges an SSF fellowship within the Strategic Research in Structural Biology programme. Financial support from the Swedish Natural Science Research Council (project 10161) is gratefully acknowledged.

Note added in proof

A closely related filter scheme was recently published by Ottiger, M., Delaglio, F. and Bax, A. (1998) *J. Magn. Reson.*, **131**, 373–378.

References

Andersson, P., Nordstrand, K., Sunnerhagen, M., Liepinsh, E., Turovskis, I. and Otting, G. (1998) *J. Biomol. NMR*, **11**, 445–450.
Bax, A. and Tjandra, N. (1997) *J. Biomol. NMR*, **10**, 289–292.
Cuperlovic, M., Palke, W.E., Gerig, J.T. and Gray, G.A. (1996) *J. Magn. Reson.*, **B110**, 26–38.
Goldman, M. (1984) *J. Magn. Reson.*, **60**, 437–452.
Grzesiek, S. and Bax, A. (1993) *J. Magn. Reson.*, **B102**, 103–106.
McCoy, M.A. and Mueller, L. (1992) *J. Magn. Reson.*, **99**, 18–36.
Meissner, A., Duus, J.Ø. and Sørensen, O.W. (1997a) *J. Magn. Reson.*, **128**, 92–97.
Meissner, A., Duus, J.Ø. and Sørensen, O.W. (1997b) *J. Biomol. NMR*, **10**, 89–94.
Nielsen, N.C., Thøgersen, H. and Sørensen, O.W. (1996a) *J. Chem. Phys.*, **105**, 3962–3968.
Nielsen, N.C., Thøgersen, H. and Sørensen, O.W. (1996b) *J. Am. Chem. Soc.*, **117**, 11365–11366.
Otting, G. and Wüthrich, K. (1989) *J. Magn. Reson.*, **85**, 586–594.
Otting, G. and Wüthrich, K. (1990) *Quart. Rev. Biophys.*, **23**, 39–96.
Pervushin, K., Riek, R., Wider, G. and Wüthrich, K. (1997) *Proc. Natl. Acad. Sci. USA*, **94**, 12366–12371.
Ross, A., Czisch, M. and Holak, T.A. (1996) *J. Magn. Reson.*, **A118**, 221–226.
Sattler, M., Schleucher, J., Schedletzky, O., Glaser, S.J., Griesinger, C., Nielsen, N.C. and Sørensen, O.W. (1996) *J. Magn. Reson.*, **A119**, 171–179.
Sørensen, M.D., Meissner, A. and Sørensen, O.W. (1997) *J. Biomol. NMR*, **10**, 181–186.
Sunnerhagen, M., Nilges, M., Otting, G. and Carey, J. (1997) *Nat. Struct. Biol.*, **4**, 819–826.
Tjandra, N. and Bax, A. (1997) *Science*, **278**, 1111–1114.
Vuister, G.W., Delaglio, F. and Bax, A. (1993) *J. Biomol. NMR*, **2**, 401–405.
Weigelt, J., Miles, C.S., Dixon, N.E. and Otting, G. (1998) *J. Biomol. NMR*, **11**, 233–234.
Zerbe, O., Welsh, J. H., Robinson, J. A., von Philipsborn, W. (1992) *J. Magn. Reson.*, **100**, 329–335.